Academic Science Journal (ASJ)
Vol. 4, No. 1, January 2026, pp. 111~118
DOI: 10.24237/04.01.501

Enhancement of polyethylene glycol with chromium oxide nanoparticles to inhibit corrosion of steel in HCl

Donia Abdulateef[1] , Safa Ahmed[2]and Haider ghrabee [3]
[1,2,3] The General Directorate for Education of Diyala

Article Info

Article history:

Received 18, 08, 2024
Revised 11, 02, 2025
Accepted 15, 10, 2025
Published 30, 01, 2026

Keywords:

Cr_3O_4 nanoparticles,
polyethylene glycol,
steel,
Corrosion.

ABSTRACT

In this work, chromium oxide nanoparticles were created using the co-precipitation approach, binary composite of chromium oxide and polyethylene glycol (PEG) in THF was created using the solution-processing method. X-ray diffraction (XRD), transmission electron microscopy (TEM), and field emission scanning electron microscopy (FESEM) were utilized to examine the morphology and determine the average size, revealing the hexagonal crystal structure of Cr_3O_4 nanoparticles. The weight loss method and a standard microscope were used to evaluate these compounds' corrosion inhibitions on steel in 5 M hydrochloric acid. The investigation into weight loss has shown that these chemicals' inhibitory efficacy changes with solution temperature and immersion time and rises with increasing weight. The different thermodynamic parameters were also computed in order to look into the corrosion inhibition process. The Freundlich adsorption isotherm governs how nanoparticles adsorb on steel surfaces in acid. The rate of the nanomaterial inhibitors was higher than 83.04%. The creation of a protected adsorption surface was thought to be the cause of the steel's potent inhibitory action. According to the computed values of the thermodynamic functions (ΔG, ΔH, and ΔS), the corrosion of the steel was endothermic, spontaneous, and non-random in the synthesized samples.

Corresponding Author:

Haider Nazar Hussein
The General Directorate for Education of Diyala
E-mail: ***haiderghrabee@gmail.com***

1. INTRODUCTION

Numerous industrial applications experience significant corrosion. Under most conditions, rusts formed by corrosion shield the metal from environments and inhibit further corrosion [1]. Corrosion consumes resources, pollutes the environment, puts safety in jeopardy, and causes direct or indirect economic loss. Still, there are certain advantages that come with rusting. Iron and its alloys are widely used as construction materials in a range of industrial applications, including the chemical, power, and petroleum sectors, due to their excellent mechanical strength, simplicity of manufacture, and low cost [2-4]Because of its many applications, steel is exposed to a variety of corrosive environments, such as acidic solutions during etching, acidic ling, acid descaling, acid cleaning, and acidification of oil well processes [5]. Significant financial loss occurs when steel alloys react easily in acidic conditions, transitioning from a metallic to an ionic state. Thus, the development of some superior corrosion-control techniques is important [6, 7]. One may categorize corrosion inhibitors based on their chemical composition, mode of operation, etc [8]. Organic corrosion inhibitors are a frequent type that has gained significant relevance because of their high level of protection, simplicity of synthesis, and relative affordability [9] [10]. The present focus of science and engineering research studies is on replacing dangerous chemicals with environmentally benign species through the synthesis, design, production, and consumption of these species [11]. The preventative strategy's reasons include adsorption on the steel surface and blockage of active corrosion sites. Corrosion damage is decreased, and the breakdown of the metal is impeded by the protective barrier that forms between the aggressive solution and the metal surface [12] [13]. In a range of solutions with acidity, organic inhibitors with heteroatoms including N, O, S, and P have been shown to function as effective corrosion inhibitors both in practice and theory [14] [15].

These atoms and their functional groups may cover vast metallic surface areas and transfer electrons to atoms' empty orbitals with ease, these inhibitors are effective because of their high polarize ability and decreased electronegativity [6].

Furthermore, sulfur-atom-containing compounds function as good sulfuric acid inhibitors, whereas metals in hydrochloric acid can be effectively protected from corrosion by organic inhibitors that include nitrogen. Sulfur and nitrogen-containing compounds work perfectly as corrosion inhibitors in both mediums [16]. Any inhibitor's effect on a particular metallic alloy in extremely acidic conditions is contingent upon the type of distinctive inhibitor film that has built up on the metal surface, as well as the quantity and makeup of adsorption centers that support the adsorption process. Generally, inhibitors with distinct heteroatoms exhibit inhibition performance in the opposite order of their electronegativities. This means that for S, N, O, and P, the inhibitors exhibit inhibition performance in the following order: O < N < S < P [17]. Acidic environments' electrochemical behavior is frequently changed when organic components are present in the acidic solutions. Otherwise, it lessens the solution's aggression. The heteroatoms of sulfur (S), phosphorus (P), nitrogen (N), or oxygen (O) are found in the most commonly utilized heterocyclic compounds, and they actively participate in adsorption centers [18].

2. METHOD

2.1 Synthesis of Cr_3O_4 nanoparticles using the Co-precipitation method.

Using the co-precipitation method, 4.0 g of $CrCl_3.6H_2O$ were dissolved in 150 mL of deionized water to create a salt solution. After gradually adding the 0.1 M sodium hydroxide solution to the precursor solution and agitating it at 40 °C, the solution's temperature was raised to 80 °C and stirred continuously for an hour to achieve a pH of about 12. After that, the precipitate was filtered and washed several times with ethanol to remove impurities and deionized water to reach a pH of 7. Following that, the precipitate $Cr(OH)_3$ NPs was gathered and dried for three hours at 80 °C in an oven.

$$CrCl_3.6H_2O + 3NaOH \rightarrow 3NaCl + Cr(OH)_3 + 6H_2O$$

The precipitated product is Calcined at 600 °C for five hours in order to produce chromium oxide nanoparticles (Cr_2O_3 NPs) [19].

$$Cr(OH)_3 \rightarrow Cr_3O_4 + H_2O$$

2.2. Preparation of Cr_3O_4 / polyethylene glycol (PEG) matrices

The matrices (Cr_3O_4 NPs and polyethylene glycol) were created by suspending (3 g) of Cr_3O_4 NPs in THF (30 mL) in Beaker (B) at room temperature and dissolving (1 g) of polymer in THF (30 mL) in Beaker (A). For roughly 45 minutes, Beaker A and B were submerged in an ultrasonic bath set at 50°C. Beaker (A) was filled with contents from Beaker (B), and the combination was immersed in an ultrasonic bath set at 70–80 °C for three hours. After the solvent evaporated, the matrices (Cr_3O_4 NPs/ PEG) as a binary composite were prepared [20].

2.3. Gravimetric measurements

Before any measurements were taken, the steel samples were carefully cleaned with distilled water, dried with acetone, and polished with various grades of emery paper up to 1200. The specimens used in the chemical investigations are in the form of squares with a thickness of 2 mm and a diameter of 2 cm. Analytical Grad 37% HCl was diluted with distilled water to create the aggressive solution (5 M HCl). Steel sample composition has weight percentage about 0.7% Impurities and the excess of iron was used.

2.4. Results and discussion

2.4.1. Corrosion effect study

This research used a 5 M HCl concentration to investigate the corrosion of steel. Using the weight loss approach, the effectiveness of Cr_3O_4/ polyethylene glycol matrix dispersion in preventing corrosion was investigated. The test samples were kept in a water bath in a beaker, then at different temperatures (303 , 333, 363, and 393 K) were estimated corrosion. In order to study corrosion, the test samples were suspended in 200 milliliters of 5 M HCl with and without different weights of Cr_3O_4/polyethylene glycol matrix as a inhibitor.

The samples were weighed before and after being immersed solution period two and four months, then each specimen were dried well, rinsed with double-distilled water, and weighed again using an electronic digital scale. The weight difference was used to calculate the total weight loss. One gram of polyethylene glycol was used in each study, along with various weights of composite (200, 400, 600, and 800 mg) acting as inhibitors.

3. RESULTS AND DISCUSSION

3.1. Characterization of nanomaterial

3.1.1. XRD analysis

The XRD patterns of the Cr_3O_4 nanoparticles (Eskolaite) and Cr_3O_4/PEG synthesized are described in Figure 1. Cr_3O_4 nanoparticles (Eskolaite) is crucial to note that the compound has a considerable degree of crystallinity, as indicated by the conspicuous peaks. With corresponding reflection planes of 10-2, 104, 2-10, 2-13, 20-4, 3-1-2, 3-14, 300, and 2-19, the hexagonal crystal system of Cr_3O_4 is accurately indexed to most of the diffraction peaks (JCPDS card nos. 00-901-6609) at 2θ: 24.54º, 33.66º, 36.25º, 41.55º, 50.31º, 58.50º, 63.57º, 65.22º, and 73.49º. The lattice constants a = 4.9510 Å and c = 13.5656 Å were obtained from the XRD observations of Cr_3O_4 nanoparticles (Eskolaite) produced via co-precipitation. Cr_3O_4/PEG composite have orthorhombic crystal system with lattice constants a=24.7578 Å b=8.4779 Å c=4.8827 Å. Cr_3O_4 nanoparticles (Eskolaite) and Cr_3O_4/PEG composite have an average size of 32.69 nm and 30.87 nm respectively, according to the Debye-Sherrer equation.[21]

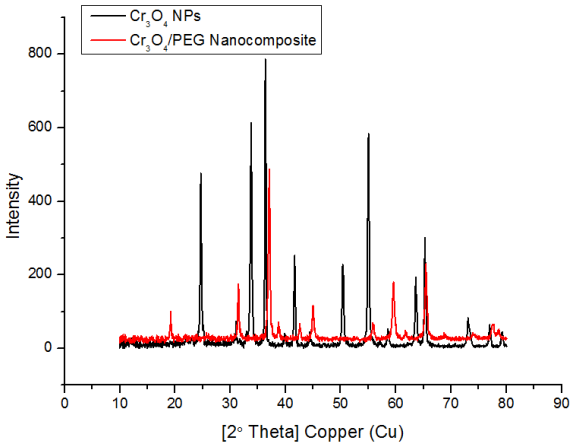

Figure1. XRD pattern of Cr_3O_4 NPs and Cr_3O_4 / polyethylene glycol matrix.

3.1.2. FE-SEM Test

Utilizing field emission scanning electron microscopy, the surface morphology of the prepared $Cr(OH)_3$ NPs is examined, Cr_3O_4 nanoparticles and Cr_3O_4 /PEG nanocomposite [22]. Figure 2 represent of $Cr(OH)_3$ NPs shows how, despite their very asymmetrical geometries, the particles aggregate to form forms that mimic cubic shapes, while having an average diameter of roughly 365.6 nm. Field emission scanning electron microscopy analysis of the produced Cr_3O_4 nanoparticle's surface shape is shown in Figure 3, it was discovered that the average diameter of Cr_3O_4 nanoparticle was 74.4 nm with fingers-shaped. While, figure 4 of Cr_3O_4 /PEG nanocomposite, Which shows complete coverage of chromium oxide nanoparticles with polyethylene glycol particles with average diameter 61.77 nm.

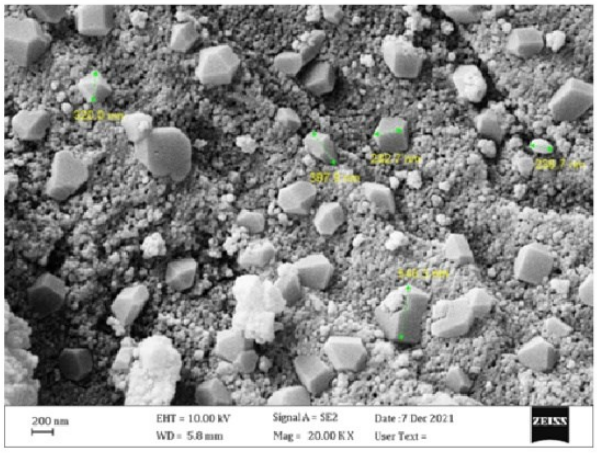

Fig.2. FE-SEM images of $Cr(OH)_3$ NPs.

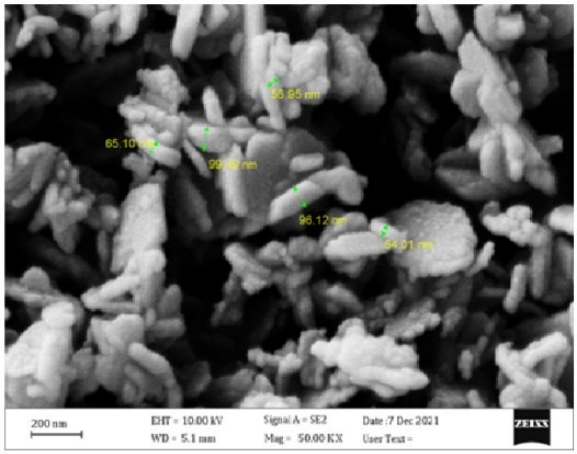

Fig.3. FE-SEM images of Cr_3O_4 NPs.

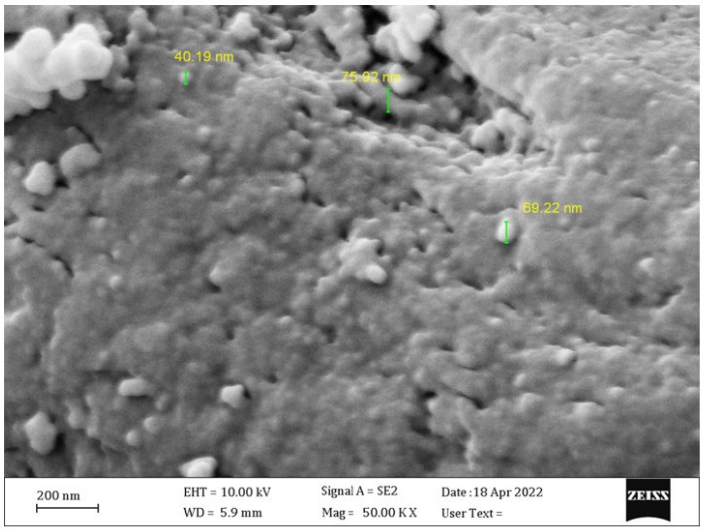

Fig.4. FE-SEM images of Cr_3O_4 / PEG nanocomposite.

3.1.3. TEM Test

TEM is frequently used to photograph and study nanoparticles in order to determine their size, shape, and morphology. Images 5 and 6 depict TEM images of the as-prepared, spherically-shaped Cr_3O_4 nanoparticles and the Cr_3O_4/PEG nanocompasite. There are some aggregated nanoparticles in addition to the individual ones. While Cr_3O_4/PEG nanocompasite generated particle sizes between 4.44 and 8.28 nm, Cr_3O_4 nanoparticle diameters were detected as ranging from 24.5 to 28.2 nm.[23]

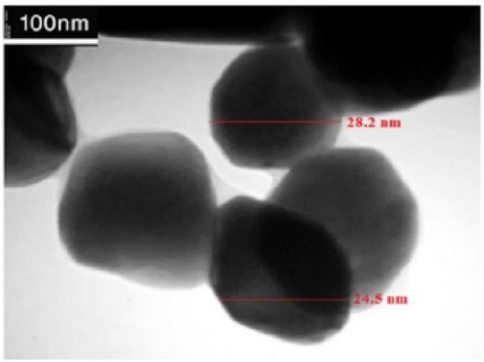

Fig. 5. TEM image of Cr_3O_4 NPs

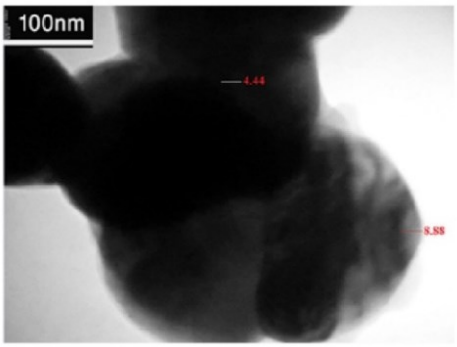

Fig. 6. TEM image of Cr_3O_4/PEG.

3.1.4. Tests for weight loss

By measuring weight loss at 303 k after two and four months of immersion, the impact of adding Cr_3O_4/PEG composite at various weights and timings on the corrosion of steel in de-aerated 5 M HCl solution was investigated. This is how inhibition efficiency (IE%) was determined [22]

$$\boldsymbol{\eta}\,\% = \frac{\mathrm{CR(Blank)} - CR(\mathrm{Inhibit})}{\mathrm{CR(Blank)}} \qquad (1)$$

$CR_{(Blank)}$ and $CR_{(Inhibit)}$ are the corrosion rates of steel samples in the absence and presence of the Cr_3O_4/PEG composite, respectively

. Degree of Surface Coverage (θ) can calculate by equation (2):

$$\boldsymbol{\eta}\,\% = \frac{W1 - W2}{W1} \qquad (2)$$

where θ is the inhibitor's degree of surface coverage and W2 and W1 are the weight losses (mg) for the steel sample with and without the inhibitor (Cr3O4/PEG). The values of the degrees of surface covering (θ) were tallied in table (1).

Table (1) and Figure 9 show the weight loss of steel in 5 M HCl at different weights with and without Cr_3O_4/PEG composite. Table 1's results make it evident that, for the Cr_3O_4/PEG composite that was tested, the steel corrosion rate values drop as the composite's weight increases for both immersion durations. At 800 mg of Cr_3O_4/PEG composite after four months, the inhibitory activity is more noticeable and reaches a maximum value of 83.04% in terms of inhibition efficiency. This research has demonstrated that the Cr_3O_4/PEG composite's capacity to prevent reductive corrosion depends on how much of it coats the steel surface.

Table 1: The results of steel corrosion by gravimetrically method in 5 M HCl both with and without the addition of Cr_3O_4/PEG composite at various weights and temperatures.

Cr_3O_4/PEG composite	Temperature (K)	Weight loss (mg)	CR (mg.cm^{-2} month^{-1})	IE%	θ
		Blank	6.010	-	-
2 Months	393	200	5.061	15.79	0.72
	363	400	4.342	27.75	0.73
	333	600	3.501	41.74	0.80
	303	800	2.834	52.84	0.82
4 Months	393	200	4.078	32.14	0.81
	363	400	3.103	48.36	0.84
	333	600	2.268	62.26	0.86
	303	800	1.019	83.04	0.89

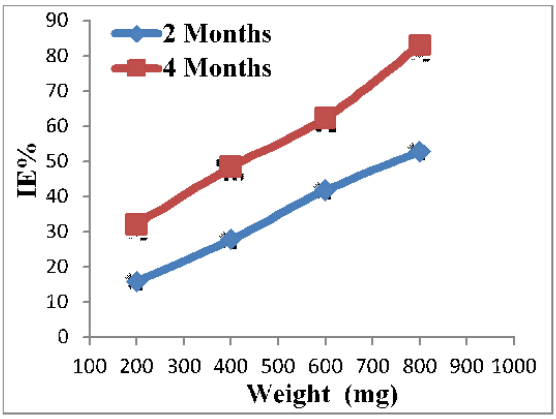

Fig.9. Inhibition efficiency with Cr_3O_4/PEG composite as an inhibitor weight at 303 k different immersion times

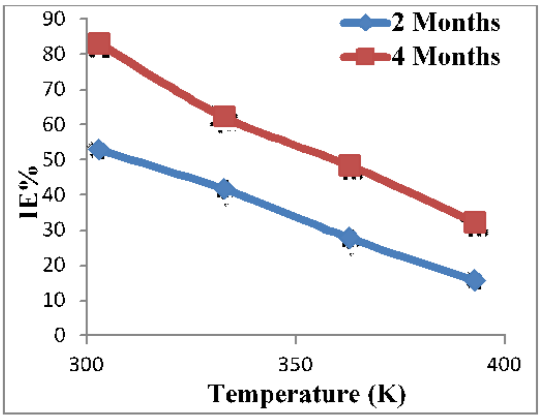

Fig.10. Inhibition efficiency with Cr_3O_4/PEG composite as an inhibitor at different temperature

Temperature has a complicated influence on the inhibited acid-steel interaction because it causes the steel surface to undergo several changes, including fast etching, inhibitor desorption, and possible inhibitor degradation. Gravimetric measurements are made at different temperatures (303–393 K) with and without Cr_3O_4/PEG composite at 800 mg for two and four months of immersion times in order to investigate the impact of temperature on the corrosion inhibition of mild steel in the acid medium and to compute the activation energy of the corrosion process. Table has the related findings (2). We observe that in both inhibited and uncontrolled acids, the corrosion rate rises with temperature. Arrhenius charts for steel corrosion rate are displayed in Figure 11. The following relation may be used to calculate the apparent activation energies:

$$\mathrm{Ln}\, CR = \frac{-\mathrm{Ea(Blank)}}{\mathrm{R\,T}} + \ln A \qquad (3)$$

A is the pre-exponential factor, T is the absolute temperature, R is the universal gas constant, and Ea(Blank) and Ea(inhibit) are the activation corrosion energies with and without Cr_3O_4/PEG.
It is observed that as temperature rises, the rate of corrosion increases in both uncontrolled and inhibited acids, and as temperature rises, the effectiveness values drop (2). Figure 12 shows the plots of the linear regression between ln (CR) and 1/T. Table (2) compiles the pre-exponential factors, A, and computed activation energies, Ea, at various inhibitor weights. The alteration of the corrosion process's mechanism in the presence of adsorbed inhibitor molecules might account for the variation in activation energy levels.

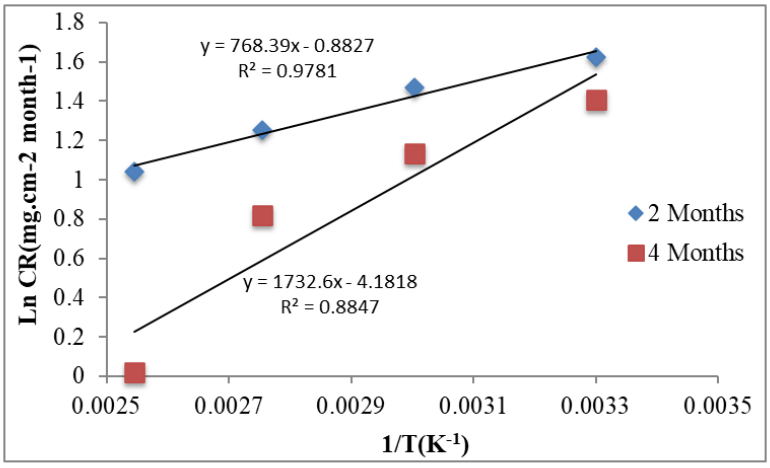

Figure12. Plots of log (CR) vs. 1/T in Presence of Cr3O4/PEG composite at a weight of 800 mg and different immersion times for steel.

Equations (4) and (5) of the transition state equation and the alternative formulation of the Arrhenius equation provide access to additional thermodynamic data (enthalpy, entropy, and free energy of the corrosion process):

$$\ln\frac{\mathrm{CR}}{\mathrm{T}} = ln\frac{R}{Nh} + \frac{\Delta S}{\mathrm{R}} - \frac{\Delta H}{R\,T} \qquad (4)$$

$$\Delta G = \Delta H - T\Delta S \qquad (5)$$

In this case, h stands for the plank's constant, N for Avogadro's number, and ΔG, ΔS, and ΔH for the activation enthalpy, entropy, and free energy, respectively. Plots of ln (ln CR/T) vs. (1/T) display straight lines with (-ΔH/R) as the slope and (Ln R/Nh + ΔS/R) as the intercept. Table (2) also displays the values of ΔH and ΔS.

Table 2. Thermodynamic parameters for corrosion of steel in 5 M HCl and in presence of 800 mg of Cr_3O_4/PEG composite as a corrosion inhibitor.

	Two months				
	T(K)	ΔG(KJ/mol)	ΔH(KJ/mol)	ΔS(J/mol.K)	ΔE(KJ/mol)
Blank	303	26.378	71	-97	53
	333	32.372			
	363	35.282			
	393	38.192			
Cr_3O_4/PEG	303	25.531	79	-84	61
	333	28.051			
	363	30.571			
	393	33.091			
	Four months				
	T(K)	ΔG(KJ/mol)	ΔH(KJ/mol)	ΔS(J/mol.K)	ΔE(KJ/mol)
Blank	303	19.466	74	-64	43
	333	21.386			
	363	23.306			
	393	25.226			
Cr_3O_4/PEG	303	13.421	89	-44	86
	333	14.741			
	363	16.061			
	393	17.381			

4. Conclusions

In this paper, the corrosion inhibition performance of polyethylene glycol with chromium oxide nanoparticles to inhibit corrosion of steel in 5M HCl solution were investigated. The conclusions are as follows:

(1) The inhibitor's inhibition effectiveness (***η*** %) increases with its weight. Many hydroxyl groups in Cr_3O_4/PEG make it a generally excellent inhibitor. Its inhibition efficiency reaches 83.04% at 800 mg of Cr_3O_4/PEG weight after four months of immersion; therefore, the inhibitory efficacy of Cr_3O_4/PEG is dependent on immersion time, which raises the activation energy of the corrosion process. The results show that when inhibitors are present, the dissolving of steel is slow because the activation energy (Ea) values for the inhibited system are larger than those for the unfettered system (Blank).

(2) Studies thermodynamics revealed of inhibitors on the steel surface by Arrhenius equation reveals that the enthalpy changes ($\Delta \boldsymbol{H}$) for all corrosion inhibitors are positive, suggesting an endothermic adsorption process. Elevated temperatures unfavorably impact the adsorption of corrosion inhibitor molecules, leading to a gradual reduction in coverage and consequently diminishing the corrosion inhibition rate. Moreover, the negative values of the entropy changes ($\Delta \boldsymbol{S}$) indicate entropy reduction during adsorption on the steel surface, implying a transition from a disordered distribution in solution to orderly adsorption, where $\Delta \boldsymbol{G}$ is the standard Gibbs free energy for all corrosion inhibitors are positive.

ACKNOWLEDGEMENTS

The authors appreciate the College of Education for Pure Sciences - University of Diyala - for using laboratories with the necessary equipment to carry out the experiment

REFERENCES

[1] H. Tamura, "The role of rusts in corrosion and corrosion protection of iron and steel," *Corrosion Science,* vol. 50, pp. 1872-1883, 2008.
[2] Y. Hou*, et al.*, "Experimental investigation on corrosion effect on mechanical properties of buried metal pipes," *International Journal of Corrosion,* vol. 2016, p. 5808372, 2016.
[3] O. Ogunleye*, et al.*, "Corrosion Characteristics and Passive Behavioral Responses," in *IOP Conference Series: Materials Science and Engineering*, 2021, p. 012234.
[4] S. Harsimran*, et al.*, "Overview of corrosion and its control: A critical review," *Proc. Eng. Sci,* vol. 3, pp. 13-24, 2021.
[5] H. Al-Mazeedi*, et al.*, "A Study of galvanic corrosion in stagnant ammonium bisulfide solution," *International Journal of Corrosion,* vol. 2019, p. 1325169, 2019.
[6] B. S. Mahdi*, et al.*, "Corrosion inhibition of mild steel in hydrochloric acid environment using terephthaldehyde based on Schiff base: Gravimetric, thermodynamic, and computational studies," *Molecules,* vol. 27, p. 4857, 2022.
[7] L. Souza*, et al.*, "Ionic liquids as corrosion inhibitors for carbon steel protection in hydrochloric acid solution: A first review," *Journal of Materials Research and Technology,* vol. 22, pp. 2186-2205, 2023.
[8] G. Palanisamy, "Corrosion inhibitors," *Corrosion inhibitors,* vol. 2019, pp. 1-24, 2019.
[9] A. A. Al-Amiery*, et al.*, "Corrosion inhibitors: natural and synthetic organic inhibitors," *Lubricants,* vol. 11, p. 174, 2023.
[10] L. Chen*, et al.*, "Organic compounds as corrosion inhibitors for carbon steel in HCl solution: a comprehensive review," *Materials,* vol. 15, p. 2023, 2022.
[11] K. Bijapur*, et al.*, "Recent trends and progress in corrosion inhibitors and electrochemical evaluation," *Applied Sciences,* vol. 13, p. 10107, 2023.
[12] F. Teymouri*, et al.*, "Passive film alteration of reinforcing steel through [MoO42−]/[RCOO−] interfacial co-interaction for enhanced corrosion resistance in chloride contaminated concrete pore solution," *Journal of Molecular Liquids,* vol. 356, p. 119060, 2022.
[13] A. Miralrio and A. Espinoza Vázquez, "Plant extracts as green corrosion inhibitors for different metal surfaces and corrosive media: a review," *Processes,* vol. 8, p. 942, 2020.
[14] B. Thirumalairaj and M. Jaganathan, "Corrosion protection of mild steel by a new binary inhibitor system in hydrochloric acid solution," *Egyptian Journal of Petroleum,* vol. 25, pp. 423-432, 2016.
[15] A. Fouda*, et al.*, "Novel porphyrin derivatives as corrosion inhibitors for stainless steel 304 in acidic environment: synthesis, electrochemical and quantum calculation studies," *Scientific Reports,* vol. 13, p. 17593, 2023.
[16] K. S. M. Ferigita*, et al.*, "Corrosion behaviour of new oxo-pyrimidine derivatives on mild steel in acidic media: Experimental, surface characterization, theoretical, and Monte Carlo studies," *Applied Surface Science Advances,* vol. 7, p. 100200, 2022.
[17] R. C. d. S. Lessa, "Synthetic Organic Molecules as Metallic Corrosion Inhibitors: General Aspects and Trends," *Organics,* vol. 4, pp. 232-250, 2023.
[18] M. Meften*, et al.*, "Synthesis of new heterocyclic compound used as corrosion inhibitor for crude oil pipelines," *American Scientific Research Journal for Engineering, Technology, and Sciences (ASRJETS),* vol. 27, pp. 419-37, 2017.
[19] S. A. Khan*, et al.*, "Green synthesis of chromium oxide nanoparticles for antibacterial, antioxidant anticancer, and biocompatibility activities," *International Journal of Molecular Sciences,* vol. 22, p. 502, 2021.
[20] A. E Sultan*, et al.*, "Synthesis of silver oxide nanoparticles (Ag2O NPs) and study their dispersion into new polymer matrix," *Journal of Nanostructures,* 2023.

[21] S. Mustapha*, et al.*, "Comparative study of crystallite size using Williamson-Hall and Debye-Scherrer plots for ZnO nanoparticles," *Advances in Natural Sciences: Nanoscience and Nanotechnology,* vol. 10, p. 045013, 2019.
[22] M. Havrdova*, et al.*, "Field emission scanning electron microscopy (FE-SEM) as an approach for nanoparticle detection inside cells," *Micron,* vol. 67, pp. 149-154, 2014.
[23] A. Alemayehu, "Size evolution of spiral magnetic structure in cobalt chromite nanoparticles," 2017.

BIOGRAPHIES OF AUTHORS

	**Donia Abdulateef** is a lecturer at The General Directorate for Education of Diyala. She received the B.Sc. degree in chemistry science from the University of Diyala in Iraq and M.Sc. degree University of Diyala in Iraq. Her research areas are Physical chemistry. She has published several scientific papers in international journals. She can be contacted at email: mscdonia33@gmail.com
	**Safa Ahmed** is a lecturer at The General Directorate for Education of Diyala. She received the B.Sc. degree in chemistry science from the University of Diyala in Iraq and M.Sc. degree University of Diyala in Iraq. Her research areas are Physical chemistry. She has published several scientific papers in international journals. She can be contacted at email:
	**Haider Ghrabee** is a lecturer at The General Directorate for Education of Diyala. He received the B.Sc. degree in chemistry science from AL Mustansiriyah University in Iraq and M.Sc. degree University of Diyala in Iraq. His research areas are Physical chemistry. He has published several scientific papers in international journals. He can be contacted at email: haiderghrabee@gmail.com